The Yale Undergraduate Research Journal

Volume 1
Issue 1 *Fall 2020*

Article 24

2020

Development and Distribution of Thermometry Hardware for the Simons Observatory

Samuel Day-Weiss
Yale University

Development and Distribution of Thermometry Hardware for the Simons Observatory

Cover Page Footnote

I would like to thank Professor Laura Newburgh and Postdoctoral Researcher Brian Koopman for their mentorship and teaching. I would also like to thank undergraduate Sebastian Tsai for his help on various elements of my projects, and the Wright Laboratory support staff for help in machining and electrical work. Finally, a big thank you to YURA and the Yale Undergraduate Research Journal for the opportunity to share my work.

STEM | Astronomy VOL. 1.1 | Nov. 2020

Development and Distribution of Thermometry Hardware for the Simons Observatory

Samuel Day-Weiss[1]

[1]*Yale University*

Abstract

The Simons Observatory (SO) is a new cosmic microwave background (CMB) experiment consisting of four telescopes. SO is being constructed at an elevation of 5,190 meters on Cerro Toco in the Atacama Desert in Chile, and is set to begin observation in 2022. SO will employ 60,000 detectors, yielding a sensitivity greater than all previous CMB experiments. To achieve low noise performance the telescope cryostats will be cooled to ~100 mK using low temperature dilution refrigerators. Measuring cryostat temperatures is essential for pre-deployment testing, telescope installation, and telescope monitoring during observation. The purpose of this project is to design, build, and test the hardware necessary for regular measurements at all temperature stages of the SO telescopes. This paper details my design of housekeeping hardware, contribution to temperature sensor calibration, and characterization of calibration discrepancies attributable to faults within my lab's dilution refrigerator.

OVERVIEW OF THE CMB

Discovery

In what started as an operation to characterize signals from an orbiting communications satellite, radio astronomers Arno Penzias and Robert Wilson encountered a persistent noise source that they could not subdue [7]. While working at Bell Laboratories in the 1960s on a horn-reflector radio antenna, Penzias and Wilson measured a signal that they did not expect, a (nearly) uniform radiation that would later be coined the cosmic microwave background (CMB) [7]. Penzias and Wilson shared their results with a group at Princeton led by Robert Dicke which had developed a theory predicting a relic thermal structure from the Big Bang. Dicke and his group suspected that, if the universe was initially hot, dense, and opaque, an isotropic background radiation would exist as remnant of that state [7]. Specifically, the sky would be radiating like an ideal blackbody, something which could be confirmed by measuring the brightness of the sky as a function of frequency. Moreover, Dicke's group predicted that this radiation would be observed today in the millimeter range of the electromagnetic spectrum, the photon wavelengths having been redshifted by the accelerated expansion of the universe. Dicke, Penzias, and Wilson's work would later be substantiated, but they themselves did not observe the CMB in its entirety. Microwave photons with wavelengths shorter than 3 cm are readily absorbed by the water molecules in the atmosphere, and the peak of the CMB spectrum occurs at a wavelength of 2 mm [7]. Penzias and Wilson's microwave antenna was designed to detect signals with a wavelength of 7.35 cm [7], and so it would not be until the launch of the Cosmic Background Explorer (COBE) satellite that the true significance of the CMB would be confirmed. COBE's data on the sky's power spectrum demonstrated that the CMB was indeed very close to that of an ideal blackbody radiating at about 2.725 Kelvin, a value in correspondence with the peak wavelength of 2 mm [7]. Evidence for the Hot Big Bang was abound, and it has since been incorporated into the standard model of physics [7].

Origins and Properties of the CMB

The cosmological history of the CMB can be divided

into three general epochs: recombination, decoupling, and last scattering [7]. The epoch of recombination was the period during which the universe transitioned from being ionized plasma to largely neutral hydrogen and helium [7]. The afterglow of this transition is essentially what we see in the CMB [8]. The epoch of photon decoupling was the subsequent period during which the rate of photon Thomson scattering became smaller than the Hubble parameter, which describes the rate at which the universe expands [7]. In this epoch photons did not travel as erratically as they did in the plasma, no longer as able to break apart atomic bonds as the universe progressively cooled [7]. Soon after, around 380,000 years after the Big Bang, the CMB photons underwent their last scattering by electrons. This epoch is designated as the epoch of last scattering, and is when CMB photons could travel freely through the universe, eventually into our detectors. The spherical surface around every observer in the universe with a radius equal to the speed of light multiplied by the time since the epoch of last scattering is called the surface of last scattering.

Although the CMB is rather uniform when looking at the sky in its entirety, observation at smaller angular scales reveals anisotropies in the temperature and polarization of CMB photons. These anisotropies are the focus of contemporary CMB experiments, and are what provide insight into the physical properties of the surface of last scattering. For example, analyzing the statistical nature of temperature fluctuations in the CMB can lead to an understanding of the density perturbations of non-baryonic dark matter in this early phase of the universe. Mapping the polarization of CMB photons is similarly enlightening. There exist two predominant forms of polarization in the CMB: linear E-mode polarization, and circular B-mode polarization. E-mode polarization is caused primarily by the aforementioned fluctuations of matter density at the surface of last scattering, while the existence of B-mode polarization is less easily explained [12]. It is hypothesized that a period of rapid expansion at the onset of the Big Bang, called inflation, would leave a background of gravitational radiation [12]. Evidence for this primordial radiation may exist in the CMB in the form of B-mode polarization, and while B-modes generated by other sources have already been documented, the search for this particular source persists.

SIMONS OBSERVATORY OVERVIEW

Instrument Overview

The Simons Observatory (SO) will consist of four new ground-based CMB telescopes. Construction of SO will occur at an altitude of 5,190 meters on Cerro Toco in Chile, adjacent to several other CMB experiments already in operation [2]. The site will have three small-aperture (~0.4 m) telescopes (SATs) and 1 large aperture (~6 m) telescope (LAT) with over 60,000 transition-edge sensor (TES) cryogenic bolometers [2].

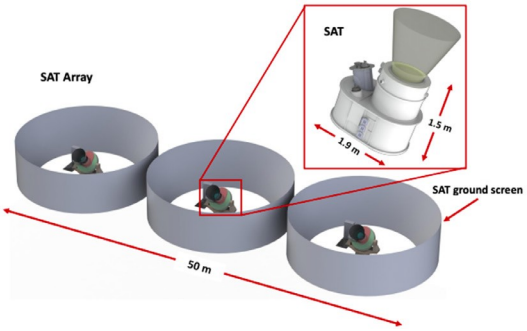

Figure 1: A conceptual image of the SAT array [4]. The ground (grey) screens protect the SATs from light contamination at the ground level. The housekeeping rack and other equipment are mounted below the boresight stage (green platforms beneath the cones pointing towards the reader) for proximity to the cryostat. The expanded image is the SAT receiver, and the cryostat is within that structure. The dilution refrigerator can be seen on the left of the receiver, inserting into the structure at an angle. Light is captured through the cone and cylinder perpendicular to the receiver.

The three small aperture telescopes (SATs) will each contain a single optics tube, housing seven detector arrays with a continuously rotating half-wave plate to modulate the polarization signal [6]. The three SATs will in total contain 30,000 detectors. Two of the SAT receivers will observe at frequencies of 93 and 145 GHz, and the other will observe at 225 and 280 GHz [6]. The SAT cryostat and supporting components and electronics will be mounted on a three-axis platform, allowing for scanning in azimuth, elevation, and rotation [6]. A diagram of the SAT Receiver mounted on the boresight stage of the telescope is shown in Figure 1, while constituent parts of the receiver are displayed in Figure 2.

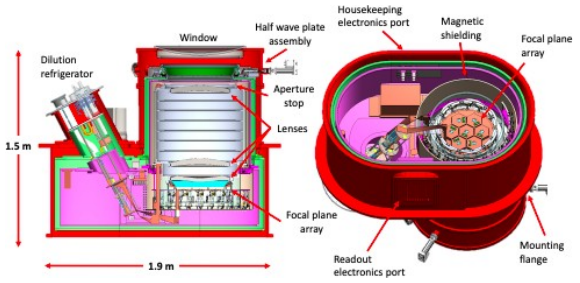

Figure 2: Left: Cross section of the SAT optics tube and focal plane array along with the dilution refrigerator. Right: Back end of receiver showing primary components in the 4K volume [4].

The large aperture telescope (LAT) is a 6 m diameter crossed-Dragone telescope, designed with an 8 degree field of view [6]. The receiver itself (LATR) can accommodate up to 13 optics tubes, each containing three anti-reflection coated silicon lenses, an array of filters, and a detector array [6]. The LAT can house 30,000 detectors [6]. Temperature requirements for detector efficiency will necessitate the cooling of roughly a metric ton of material to 4 Kelvin, and over 100 Kg to 0.1 Kelvin. As will be discussed, it is important to monitor the cooling of such a massive object to ensure that the detectors are operating under optimal conditions. A model of the LAT is shown in Figure 3, and a picture of the inside of the LATR is displayed in Figure 4.

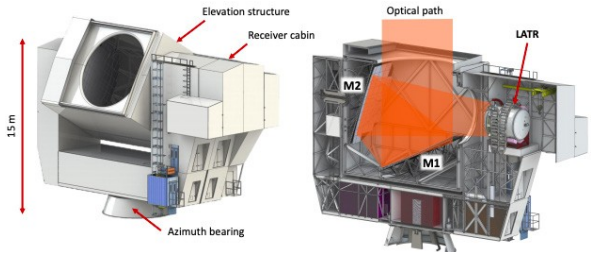

Figure 3 [4]: Model of the LAT. The optical path shown on the right details the path of light into the receiver (LATR). The LAT housekeeping equipment will be located within this structure.

Science Objectives

Through the observation of a wide range of angular scales, SO will shed light on some of the most important mysteries in cosmology. The LAT will survey 40 percent of the sky with arc-minute resolution, hoping to improve our understanding of (among other things) the sum of neutrino masses, the number of relativistic species, the dark energy equation of state, dark matter properties, and the astrophysics of galaxy clusters [1]. The SAT will perform a deep, degree-scale survey of 10 percent of the sky, aiming to continue efforts to detect primordial B-mode polarization, which may provide information about the energy scale of universal inflation [1]. SO will operate with up to ten times the sensitivity and five times the angular resolution of the Plank satellite, increasing the mapping speed of current CMB experiments by roughly an order of magnitude [6]. SO will measure CMB temperature and polarization fluctuations in six frequency bands from 27 to 280 GHz, with the goal of rapidly expanding our capabilities in CMB science while informing the design of future CMB experiments [6].

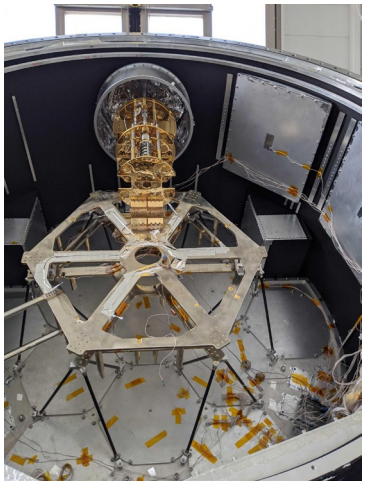

Figure 4: The LATR with its dilution refrigerator (DR) (gold plated) and cold plate (the hexagonal plate to which the TES bolometers will be thermally coupled). From the top gold plate down (moving towards the photographer): the 4K stage, 1K stage, and 100 mK stage of the DR. RX-102A thermistors can be seen on the hexagonal plate, one of which is on the bottom of the small central circle (the sensor is a small, copper colored circle with a white lead extending from it). RX-102As will be placed throughout the cryostat to monitor the bath temperature.

Schedule

The first SAT (SAT-1) is scheduled to be deployed in the fall of 2021, and will see first light in 2022 [6]. SO plans to begin a 5 year survey in 2022 with the goal of extending its operation time [6]. This extension, titled 'SO-Enhanced', may occur with the potential addition of SO to the larger CMB-S4 project [6].

OVERVIEW OF THERMOMETRY HARDWARE

For ground-based CMB instruments, TES bolometers have hit an irreducible noise floor due to signal contamination from the atmosphere. As such, SO will improve CMB observation by deploying an unprecedented number of multiplexed detectors, over 60,000 AlMn alloy TES bolometers with a target critical temperature of 160mK (where they

transition to become a superconducting material) [3]. During data acquisition TES bolometers are voltage biased so that they remain on their critical temperature, and it is only at this temperature that they function [4]. TES Bolometers at their core are sensitive thermometers (thermistors), and near their critical temperature small deviations in their temperature yield large, measurable changes in their resistance. It is important that the TES bolometers be able to heat up to make measurements, but it is equally important that this heat be dissipated in order to maintain the critical temperature. This dissipation is managed by thermally conductive "legs" connecting to the bath (cryostat), the geometry of which are specific to the dissipation needs [4]. If too much heat is deposited on the TES bolometers this may "saturate" them, i.e. push them off of their transition temperature and render them dysfunctional. Saturation can occur from the CMB and the surrounding atmosphere, but also from thermal emission from the telescope mirrors and refractive optics, in addition to the optics tubes and the telescope itself [4]. The mitigation of thermally induced systematic errors is essential given the sensitivity of the detectors to loading, but is made difficult by the amount of mass on the telescope that must be cooled to less than 4K. My work with SO housekeeping hardware primarily involved methods to address this challenge.

The power required for saturation is in fact intimately related to a quantity called the bath temperature: the temperature of the cryostat within which the detectors are placed. SO receivers will operate at a bath temperature of 100 mK, the choice of which is fundamentally related to thermal noise: the lower the bath temperature, the lower the thermal noise, and the lower noise detectors that can be used. Monitoring this bath temperature during telescope testing, cooldowns, and operation is critical to the observatory. Beyond understanding the saturation behavior of the TES bolometers, monitoring the bath temperature during telescope operation serves as a basic measure of functionality. Higher than expected bath temperatures would indicate problems with the cryostat, and quickly identifying and rectifying these problems ultimately enables the experiment to run for longer, uninterrupted durations. The bath temperature will also indicate whether the detectors are working properly, and in extreme cases (if the bath temperature is close to the critical temperature of 160mK, for example), may be cause to disregard data. The essential hardware for bath temperature monitoring is summarized in the sections below.

Bluefors LD400 Dilution Refrigerator

In general, dilution refrigerator (DR) systems are the only systems that provide continuous cooling power at temperatures below 300 mK [9]. The Bluefors LD400 employs a pulse tube to reach a temperature of 4 K after which the thermodynamic properties of a Helium-3-Helium-4 mixture are utilized to cool to the desired bath temperature of ~100 mK [9]. The LD400 has multiple temperature stages, constructed with concentric circular shells, as shown in Figure 4. The Bluefors LD400 DR is the cooling mechanism for all of the SO telescopes, and one will be used to cool each of the receivers. My lab, the Newburgh lab, along with a variety of the other testing institutions for SO, possess an LD400 and use it to both test elements of the receivers and prepare components which will eventually be placed in the cryostats.

Lakeshore DT-670 Silicon Diode and RX-102A Ruthenium Oxide RTD

The DT-670 and RX-102A are the primary sensors employed to monitor the temperature of the telescope cryostats. The DT-670 relies upon the temperature dependence of the forward voltage drop in a p-n junction biased at a constant current, and provides sensitivity for a temperature range from 1.4 K to 500 K [11]. The RX-102A is a thick-film resistor consisting of bismuth ruthenate, ruthenium oxides, binders, and other compounds [10]. Unlike many other materials, ROXs have a negative temperature coefficient, meaning that as they cool, their resistance increases. This unique property allows ROXs to be sensitive down to temperatures as low as 50 mK [10]. As indicated by their temperature ranges, the DT-670 is used to monitor the first stages of cooling for the telescope cryostats, recording data for temperature ranges up to room temperature. The RX-102A sensors are used for colder temperatures and among other places will be installed on the

plates housing the detector arrays. Although it is difficult to see them, various ROXs are displayed in Figure 4 on the hexagonal cold plate to which the bolometers will be thermally coupled. The Newburgh lab has worked heavily with both of these sensor types to prepare, calibrate, and distribute them to our collaborators.

Lakeshore LS240 and LS372

The Lakeshore LS240 and LS372 serve as the readout devices for the DT-670 and RX-102A. The LS240 is a DIN rail, rack-mountable device which can read out temperatures from 1-800 K, while the LS372, also rack-mountable, can make measurements down to and below 100 mK. The LS372 is accompanied by a 16 channel scanner which multiplexes the readout, switching between the connected thermometers. The location of the LS240 and LS372 devices differ between the SAT and LAT. For both types of telescope, shielded leads will transmit the temperature data from within the cryostat to a warm break-out box (WBOB). For the SAT, this WBOB will be mounted to the side of the receiver, while on the LAT it will likely be located within the building complex that houses the detectors. From the WBOB, data will be transferred to the appropriate read-out device, given the temperature at which each thermometer it connects to is measuring. On the SAT, this secondary step of data transmission will be to a 19 inch rack bolted underneath the boresight stage of the telescope, called the housekeeping rack. This rack will contain all of the housekeeping devices for the telescope, including thermometry read-out devices and the network and timing devices required for operation of the LS240s and LS372s. On the LAT the rack will be of the same construction, but will once again be placed within the building complex. Much of my work has involved negotiating the layout for this rack, as well as designing and constructing the necessary enclosures within which thermometry/timing hardware will be installed.

DEVELOPING A DEPLOYABLE THERMOMETRY SYSTEM FOR THE SO TELESCOPE ARRAY

My work with SO thermometry hardware can be divided into two main categories: the development and construction of SAT-1 housekeeping hardware, and the calibration of RX-102A (ROX) sensors. It should be noted that the focus of this report is on the SAT-1, the first telescope which will be deployed, but that my responsibilities also pertain to the LAT. The two other SATs will have the same hardware preparations as the SAT-1, and my upcoming work will, among other things, involve preparation for the SAT-2, SAT-3, and LAT.

Development of Thermometry/Timing Enclosures for the SAT-1 Housekeeping Rack

The housekeeping system is a collection of hardware and an overarching network that tracks the behavior and performance of the observatory during operation. The housekeeping hardware will be placed on a 19 inch rack bolted to the boresight stage of the SAT (underneath the green stage depicted in Figure 1). Much of my work has involved the design and construction of rack-mountable enclosures for the thermometry and timing housekeeping hardware. More recently my work has expanded to include design considerations for the whole rack. In 2019 I proposed a layout for the timing/temperature enclosures (Figure 5), and although design requirements have since necessitated major layout changes, the proposal gives an idea about the kind of space needed for this hardware and the types of devices that will be included.

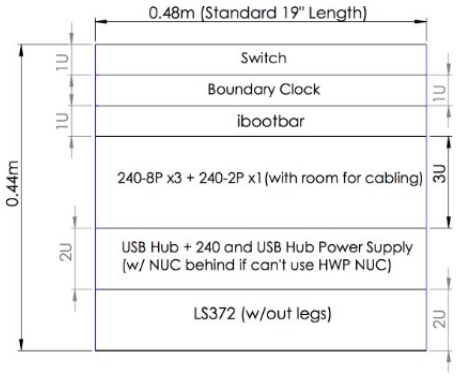

Figure 5: 2019 Proposal for thermometry/timing layout on the SAT-1 housekeeping rack (1U is ~1.75 in.) The housekeeping rack layout has since been updated as of Spring 2020, but this diagram gives a sense of the rack size needed and displays many of the components that will be installed.

The Atacama desert's relatively extreme environment necessitates careful planning for the deployment of electrical equipment. The SAT-1 housekeeping rack will be shielded from downward precipitation (primarily snow) by the boresight

stage, but this stage also tips as the telescope rotates, and thus does not protect the rack from sideways precipitation, nor from the accumulation of water or dust. Operational temperature requirements for the hardware are also essential considerations when installing electronics in close quarters, and as will be discussed below, ensuring proper cooling is a primary concern. At the time of my initial layout proposal, final decisions about the weatherproofing of the housekeeping rack had not been made, and so I developed a prototype enclosure containing much of the thermometry electronics that would be installed at the observatory site.

Development of the SAT-1 LS240 Power Supply Unit Enclosure Prototype

The LS240 Power Supply Unit Enclosure Prototype (LS240 PSU) contains a power supply for both the LS240s themselves and for a USB hub meant to read out the data collected by the LS240s. This data is then re-directed out of the box to an ONLOGIC ML100G-10 NUC computer. The following paragraphs detail the construction of the LS240 PSU prototype, and, although this design is not what will be deployed, it outlines the general process of construction that will be replicated for the final thermometry enclosure.

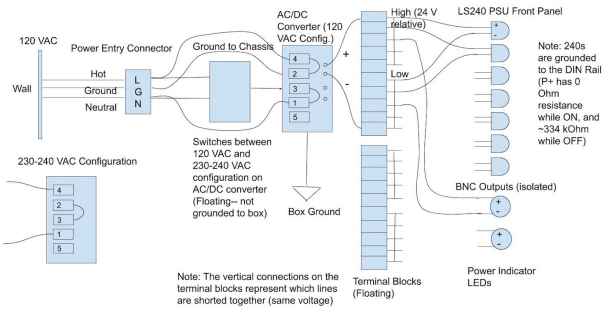

Figure 6: Electrical connection diagram for the SAT-1 LS240 PSU prototype.

Initial design for the LS240 PSU involved my planning electrical connections (Figure 6), and developing a Solidworks model (Figure 7) which was sent to a company specialized in enclosure construction. Once fabrication of the enclosure was completed, the LS240 PSU was sent to our lab for assembly. I checked the enclosure for design flaws, altered accordingly, and completed the electrical connections between components using the circuit diagram in Figure 6. A notable component in this design is a DPDT switch which changes the configuration of the AC/DC converter from compatibility with a 110 VAC supply to a 220 VAC supply. The observatory site in Chile will be designed for compatibility with 220 VAC, while all of the test institutions in the US will operate at 110 VAC. In order for any of the housekeeping electronics to be site-deployable, preparation for this voltage change is required.

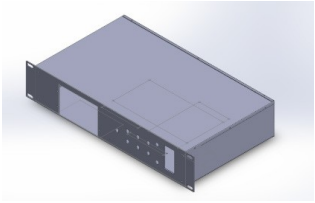

Figure 7: Solidworks prototype for the SAT-1 LS240 PSU.

The next phase of the project was testing. I tested the electrical connections first by following the logic of the circuit diagram. In preparation for the possibility that the entire housekeeping rack be exposed to the outdoors, I then sealed the LS240 PSU with a weather-proof neoprene foam. I successfully filled the seams with a combination of the neoprene foam, aluminum tape, and an aluminum metal plate, and it is to be seen how often the sealants will need to be replaced (hopefully never if the adhesive of the neoprene foam stays strong).

Figure 8: SAT-1 LS240 PSU (red box) undergoing testing. The LS240 PSU can be seen here connected to 1 LS240-2p and 3 LS240-8ps, replicating the experimental conditions for the SAT-1.

The final step of testing for the LS240 PSU prototype involved the recreation of the conditions needed on the actual SAT-1. I connected the power supply outputs on the front panel of the LS240 PSU to four of the LS240 devices, which in turn connected to a USB hub, also located in and powered by the box. This final test was passed, and the LS240 PSU has since been sent to UCSD for integration into their set-up with the SAT-1. It is being used to visualize the layout of the housekeeping rack, and will eventually be replaced with my next design, detailed in the following section. An image of the completed LS240 PSU undergoing testing can be seen in Figure 8.

Final Design Plans for SAT-1 Thermometry/Timing Hardware

In Spring 2020, I convened with collaborators from UC Berkeley and UCSD to finalize design plans for the SAT-1 housekeeping rack. We decided that the back and sides of the rack would be fully enclosed for weather protection, while the front would be open (but weather proofed as much as possible) to allow for access to the electronics/connections. These protective requirements, an updated list of hardware going into the rack, and my need to compensate for other devices in the thermometry enclosure prompted massive design changes to the original LS240 PSU. Development of the new enclosure is an ongoing project, but my latest design is displayed in Figure 9 with labels for the devices within, and the connection diagram can be found in Figure 10. While the new enclosure will have some of the same devices as the LS240 PSU (power supply, USB hub), most of the contents are new, and much of the external connection chain described in the LS240 PSU section will now be contained within the enclosure. The enclosure itself is 4U (the LS240 PSU was 2U) and will contain devices essential to the thermometry, continuously-rotating half wave plate (CHWP), and calibration grid loader housekeeping systems. The continuously-rotating half wave plate will be placed in front of the SAT-1 optics tube to modulate the polarization of the incident light and ultimately reduce atmospheric contamination of the desired signals [5]. The calibration grid loader is a circular device with an array of parallel wires which will be placed in front of the SAT-1 cryostat. The grid loader rotates and calibrates for relative polarization angle sensitivity.

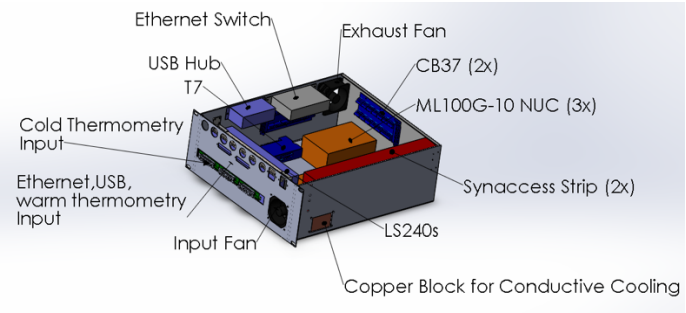

Figure 9: Solidworks design for the final housekeeping thermometry hardware enclosure.

Within the new thermometry enclosure, two Synaccess network controlled power strips, which are compatible with 110 and 220 VAC, will replace the LS240 PSU linear power supply, removing the need for the DPDT switch and allowing for easy connection to DC power adapters for the electronics. Three ONLOGIC NUC computers will be contained in the enclosure, one to read out cold thermometry data (from the RX-102As and DT-670s), power the USB hub, and read out data from the calibration grid loader, one to monitor the timing system of the CHWP, and one to read out the CHWP actuators and the star camera. Both the CHWP and grid loader will have housekeeping enclosures installed on the housekeeping rack. Four Labjack devices will be included in the thermometry enclosure (the T7, Mux80 and two CB37s), all of which will be used to read out warm thermometry data from thermistors installed outside of the telescope cryostat. The LS240s will go inside of the enclosure instead of standing alone on the rack (as originally planned with the LS240 PSU) and will channel data to the USB hub which connects to one of the NUCs. A copper block which will be thermally coupled to the housekeeping rack for cooling is included, which can accommodate heat straps sized to match power usage specs for the most dissipative components (NUCs and DC power adapters). Finally, two fans, one input and one exhaust, will be installed to help cool the electronics. The selection of the fans and the direction of airflow within the enclosure was an important consideration, especially because the NUC computers contain no internal fans, and many of the other electronics are sensitive to deviations from room temperature (~25C). I calculated that the fans would need to remove about 7 cubic meters of air per minute to ensure safe operation of the electronics on a hot day in the Atacama, and determined that the air flow should run across the width of the NUCs parallel to cooling fins meant to dissipate heat. It is ultimately most important to ensure proper functioning of the NUCs and LS240s, and future work will involve testing the cooling system while operating all of the electronics in the completed enclosure.

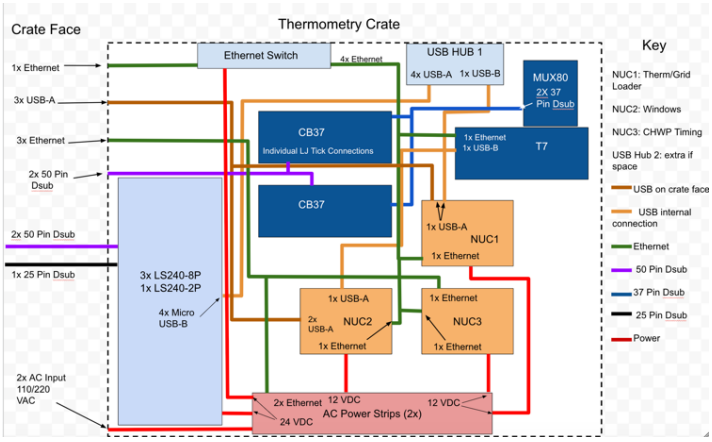

Figure 10: Connection diagram for the final housekeeping thermometry hardware enclosure. Some of the hardware described in the LS240 PSU section is shown here, now inside of the enclosure. There will be almost no replication of the connections on the electrical diagram for the LS240 PSU because most of the components included in that diagram are no longer required.

In addition to this enclosure, thermometry housekeeping will also include two LS372s. For timing, a boundary clock will be installed within a 1U enclosure, which will provide the timing synchronization for the rack, a part of an observatory-wide timing network. Future work will involve finalizing the enclosure for the boundary clock. The rest of the work for this final thermometry enclosure will involve much of the same process as for the LS240 PSU. Once the physical enclosure model is finalized I will submit the design for construction, finalize the connection diagram, assemble the enclosure, test it under experimental conditions, and weather-proof it. The assembly and testing will then need to be completed for the enclosures on the SAT-2 and SAT-3 in preparation for their deployment in the coming years, and an entirely new design will be needed for the LAT.

DESIGN OF THE SAT-1 HOUSEKEEPING RACK ENCLOSURE AND COOLING SYSTEM

My most recent work has involved designing the weather proof enclosure for the housekeeping rack, in addition to the cooling system meant to accompany the cooling methods for all of the independent enclosures/devices. The collaborators designing the CHWP and calibration grid loader housekeeping enclosures sent me their Solidworks models, and I made a rendition of the housekeeping rack with a proposed final layout, depicted in Figure 11. Figure 11 is a model of the actual rack frame depicted in Figure 12. Moving down the rack in Figure 11, the Ibootbar is a network controlled power switch which will provide power for several of the rack components, the Network Switch will provide connection to the observatory's overarching network and allow for housekeeping data transmission, the DR LS372 will provide low temperature readout for the dilution refrigerator in the cryostat of the SAT-1, the Thermometry Crate is the enclosure that I designed, the CHWP Crate controls the motor and readout for the CHWP, the Grid Loader Crate controls the calibration grid loader, and the Thermometry LS372 provides read out for bath temperature measurements. Preliminary designs for top/bottom and side covers are shown. The top/bottom covers each have slots for 6 120mm x 120mm fans for cooling. The configuration of the components in the rack optimizes air flow down the back and sides so as to reach all of the electronics. Future work will involve testing this air-cooling method.

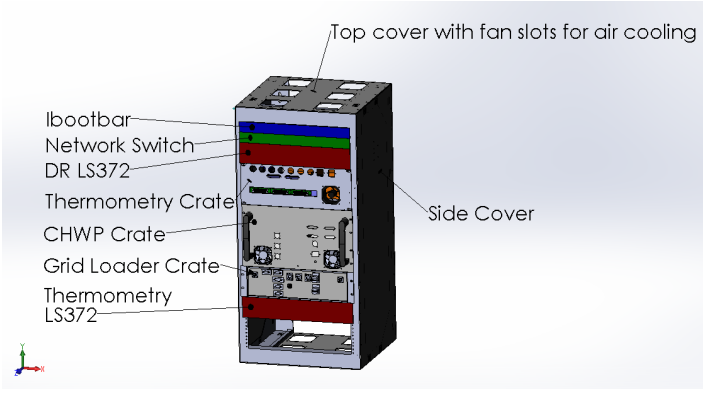

Figure 11: Solidworks model for the SAT-1 housekeeping rack. The thermometry hardware enclosure can be seen at the top labeled "Thermometry Crate", and two LS372s are seen in red.

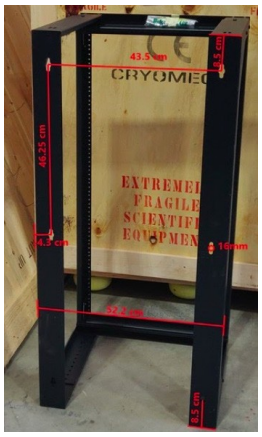

Figure 12: The actual housekeeping rack to be installed on the SAT-1 boresight stage. The Solidworks assembly shown in Figure 11 is a model of this rack.

In general, cooling for the housekeeping rack will be achieved through a combination of coupling to the cooling power of another equipment rack under the boresight stage of the SAT-1, air cooling, and conduction. Air cooling will occur by flowing chilled air down the sides and back of the rack. Coupling to the cooling power of the other equipment rack may provide this chilled air. Cooling through conduction necessitates a thermal connection between all of the most temperature sensitive devices to the boresight stage of the SAT-1, and would be done through the installation of copper plates (see Figure 9) and heat straps on the enclosures and rack. I will have to design these thermal connections. I have already collected information about the power consumption and temperature sensitivity of the devices in the rack, and future work will involve finalizing the design for the overarching cooling system, in addition to weatherproofing the rack against dust and water collection.

CALIBRATION OF THE LAKESHORE RUTHENIUM OXIDE SENSORS (ROXs)

The Calibration Process

The Newburgh Lab is responsible for calibrating hundreds of temperature sensors, an endeavor that is still under way. The following is a description of the calibration process developed by members of the lab other than myself, however I have participated in almost every part of this process at various times. Aspects of the calibration process that I designed are explicitly mentioned as such.

In order for the ROXs that will be placed near the detectors to accurately portray temperature, they must be calibrated to a sensor with incredibly well known properties. Lakeshore Cryotronics provided our lab with this well-known sensor, a calibrated ROX meant to be the calibration standard for the rest of our RX-102A thermistors. To perform calibration, the calibration standard and up to 24 un-calibrated ROXs are placed on a copper plate on the 100 mK stage of an LD400 Dilution Refrigerator (DR). The DR is then cooled while taking data with the thermometers such that calibration files for every sensor can be made. The entire process of calibration can be broken into three stages: Pre-cooldown, cooldown and warmup, and post-warmup. An image of the copper plate in the DR can be found in Figure 13, and a diagram of this plate with a layout for one of our cool downs is displayed in Figure 14.

For the pre-cooldown stage, the DR is opened and thermometers already in the fridge are removed and prepared for distribution to our collaborators. New ROXs are then placed on the copper plate and their physical location in the fridge is documented. The DR is then closed again, and various preparation steps (for example pumping on the vacuum can of the DR and the refilling of the liquid nitrogen dewar) are completed before cool down can begin.

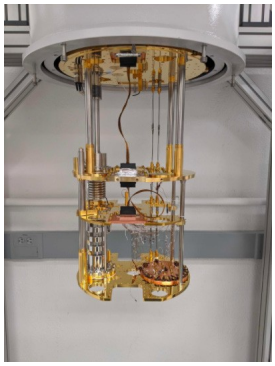

Figure 13: The Bluefors LD400 dilution refrigerator used for ROX calibration. The circular copper plate hosting the uncalibrated ROXs (and the 1 calibrated one) is on the bottom (100 mK) stage of the DR. Also shown are the heater (in the center of the copper plate), the 4K stage (top gold plate) and the 1K stage (next golden plate down). The heater lines likely causing calibration discrepancies (see following section) are located in the coils connecting the center of each plate, directly adjacent to the ROX readout wires.

During the cool down and warm-up stage, a 24 hour period is taken to cool the DR from room temperature to around 50 mK, during which data is taken for the upper temperature range of the ROX calibration curves (less data points are needed for the upper ranges because we require these sensors to be the most accurate at sub-Kelvin temperatures). Once the base temperature is achieved, the DR is prepared for a process called "servo-ing". As demonstrated in Figure 15, to gather sufficient data points at the necessary temperature steps for calibration, a heater located on the 100mK copper plate is used to deposit power, slowly increasing its temperature and plateauing for data collection. Each sensor is measured at every temperature step for 2 minutes at a rate of 4 Hz. The temperature read out by each ROX is averaged over these 2 minutes before it is compared to the temperature measured by the calibration standard. The first temperature range is from 50-240 mK in step sizes of 5 mK, and the second is from 260-800 mK in step sizes of first 20, 30, and then 35 mK. Once this process is complete, the fridge is returned to base temperature before initiating a warm-up. Python scripts written to access the data and write calibration files are run, including a merging script that I wrote to combine and format the calibration files from the different temperature step ranges mentioned above. Once the calibration files are completed for each ROX, they are uploaded to the LS372s where they are monitored for inconsistencies during the warm-up. Only after this upload can the DR be warmed to room temperature again.

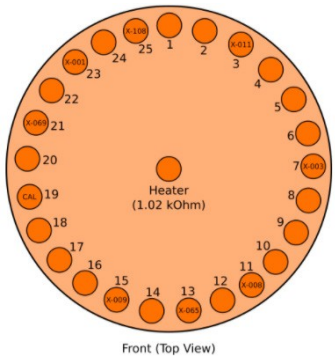

Figure 14: Diagram of the 100 mK stage copper ROX plate. Each smaller circle on the perimeter of the plate is an RX-102A sensor (labeled with X-001, etc.). X-001 was the first ROX to be labeled and stays in the DR for all cooldowns to monitor the consistency of calibration. X-108, as an example, is the 108th sensor to be labeled; the numbering for ROXs goes into the hundreds. CAL is the Lakeshore calibrated thermometer. The heater in the middle provides heating for servo-ing.

Finally, in the post-warmup stage of calibration, once it is confirmed that the calibration curves are accurate to the behavior of every ROX, the curves are uploaded to the Simons Observatory Github where they can be accessed by SO collaborators. The process then repeats.

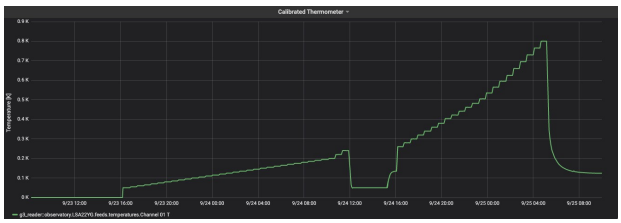

Figure 15: Calibrated ROX temperature vs. time for a calibration servo in the Newburgh lab DR. The first series of steps is from 50-240 mK, and the second is from 260-800 mK.

Troubleshooting Calibration Discrepancies Between the Bluefors and Lakeshore Calibrated ROXs

A recent focus of my work has been in response to ROX calibration inconsistencies observed by collaborators at the University of Pennsylvania. UPenn noticed that the calibrated ROX thermometer provided with their Bluefors DR differed by as much as 10 mK from the thermometers that we had calibrated. After some investigation, the postdoctoral researcher in our lab noticed similarly odd differences between the thermometer pre-installed in the Bluefors DR and the calibration standard thermometer provided by Lakeshore. This revelation poses a number of difficulties, most notably that our previously generated calibration curves are likely incorrect.

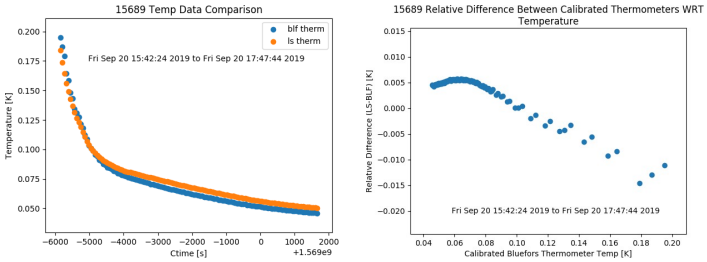

Figure 16: (Left) Example LS/BLF temperature comparison for the cooling section of a cool down: temperature of the Bluefors and Lakeshore calibrated thermometers vs. Ctime, the number of seconds since January 1, 1970 at midnight UTC (this is a standard time reference in computer applications, and the actual date is written in text in the middle of the figure). "15689" is the first five digits of the Ctime for the data frame, roughly corresponding to the day. This figure depicts the final stage of the DR cooldown as it reaches its base temperature of 50 mK, and the two calibrated thermometers match one another reasonably well. (Right) Example relative difference plot for the cooling section of a cool down: the difference in temperature between the Bluefors and Lakeshore calibrated thermometers as a function of the Bluefors sensor temperature. As compared to Figure 17, the differences here are clearly less significant.

Initial inquiries into the issue were inconclusive, and so I wrote a script to analyze the last 1.5 years of our lab's DR cool down data in order to identify patterns of difference between the Lakeshore (LS) and Bluefors (BLF) calibrated thermometers. I started by making general comparison and relative and absolute difference plots for each day of data, in addition to similar plots for data across the entire time frame. The goal was to identify patterns on small timescales, and to additionally determine if the differences between the thermometers converged or diverged across all cool downs.

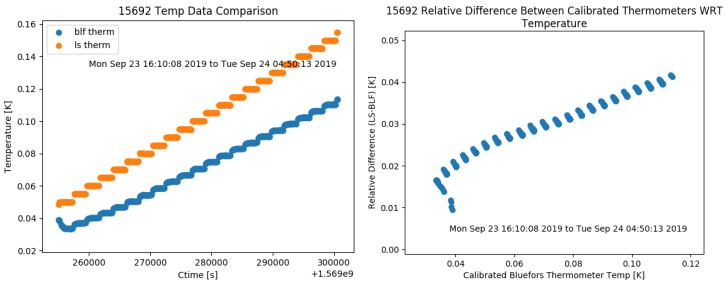

Figure 17: (Left) Example LS/BLF temperature comparison for the servo section of a cool down. See Figure 16 for information on the axes labels and title. During this stage of the cooldown the heater depicted in Figures 13 and 14 is used to increment the temperature of the ROXs. As temperature increases the difference between the Bluefors and Lakeshore calibrated thermometers increases, suggesting a correlation between heater use and calibration discrepancy. (Right) Example relative difference plot for the servo section of a cool down. Differences between the calibrated ROXs with respect to the Bluefors ROX are significantly larger during servo than either cooling or warm-up.

On smaller time scales patterns in differences became immediately apparent. I cross referenced the dates of each pattern with a detailed log of every cool down that our lab had performed. I then matched the patterns to particular sections of the cool down process. There were three sections that I identified: cooling: when the DR is first cooled to its base temperature, servo: when the heater on the copper plate on the 100 mK DR stage is used to warm to specific temperatures and calibration data is taken, and warm-up: when an internal script is run to warm the DR back to room temperature. Examples of the plots generated during each of the sections are displayed in Figures 16-18.

As suggested in Figures 16-18, differences between the LS and BLF thermometers are relatively similar in the cooling and warm-up sections of the cool downs, while the servo sections produced significantly higher differences. In some cases servos produced differences of up to 60 mK at 100 mK, an unacceptable margin of error for thermometers we are using primarily to monitor surfaces at sub-kelvin temperatures. In the servo section of every cool down the only difference between the physical environments of the BLF and LS ROXs is their proximity to the heater being used. There are two heaters installed in the Newburgh DR: one pre-installed by Bluefors, and the other installed by our lab for calibration (see Figures 13 and 14). The greatest discrepancies in read out occur during servo, when our own heater is used to warm the 100mK cold plate. This suggests that the heater is in some way causing the calibration discrepancies. If this is the case, it is additionally possible that higher frequency noise from the lines connecting the heater to electronics outside of the fridge is contaminating the temperature data in an adjacent wire attached to the calibrated ROX. This last point is a related, but potentially separate hypothesis to explain the calibration discrepancies. Troubleshooting for both the combined hypothesis, and this final hypothesis alone, is later described.

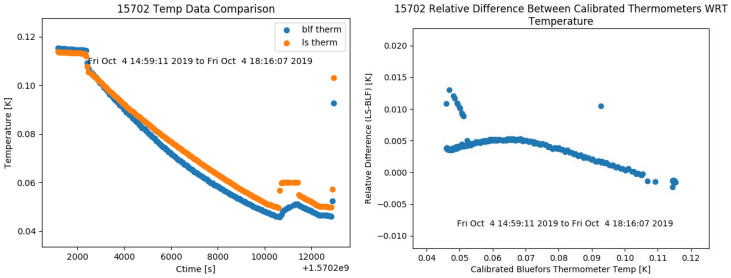

Figure 18: (Left) Example LS/BLF temperature comparison for the warm-up section of a cool down. During warm-up a script is run to return the DR to room temperature. Like during cooling, the Bluefors and Lakeshore calibrated thermometers exhibit similar behavior during warm-up. It is important to note that the heater on the 100mK copper plate is not used to warm the DR during this section of the cool down. (Right) Example relative difference plot for the warm-up section of a cool down. The difference between the calibrated ROXs as a function of the temperature of the Bluefors ROX is very similar to the cooling section.

Although it is probable that our heater is the source of the calibration discrepancies, the exact properties of those discrepancies remain unknown. The overarching goal of this analysis is to re-calibrate the "calibrated" LS thermometer, and to adjust all of the other calibration files accordingly. Under ideal circumstances, the discrepancies observed during servo-ing would be consistent across all cool downs, and this

adjustment of calibration files would only involve a simple curve fit. However, upon looking at servo data across several of the cool downs, it is obvious that the re-calibration will not be this simple. Figure 19 overlays servo data for 7 cool downs, and as we can see there are two behaviors that emerge, one with significantly higher differences than the other as a function of the temperature of the Bluefors thermometer. The problem is that these two paths are not chronologically related, and adjacent cool downs seem to exhibit radically different behavior. Upcoming work by members of our lab will be to identify what was happening during each of those cool downs, with the hope of solidifying our understanding of the calibrated thermometer differences during servo.

In the midst of the pandemic both graduate students and postdoctoral researchers have been allowed to return to do lab work under restricted schedules. While I have not been allowed to be a part of this return, members of our lab have begun to implement a variety of tests on the DR set-up to further evaluate the BLF/LS ROX calibration differences. Once this is complete, we will be able to finish the rest of the ROX calibration runs without error, in addition to fixing the calibrations for previously calibrated sensors. Members of the lab will test each of the following solutions separately: 1.) Responding to a recommendation from Lakeshore about grounding the DR components, they will ensure that there are no shorts between the gas handling system and the other elements of the DR. 2.) They will extract and rewire the lines that provide power to the heater at the center of the 100 mK copper plate to distance them from the calibrated ROX (these lines have always been directly next to the wires that carry ROX data, so if they are noisy, there is no surprise that they have caused calibration discrepancies). 3.) Finally, if neither of the other two measures entirely compensate for the discrepancies, they will place a cryogenic low-pass filter in front of the calibrated LS sensor, something that the Bluefors sensor already possesses. This would alleviate complications resulting from high frequency noise emitted (potentially) by the heating lines. Another possible solution would be to use the data from the BLF thermometer to re-calibrate all of the ROX sensors, something that would alleviate the need to cool down each of the sensors for a second time.

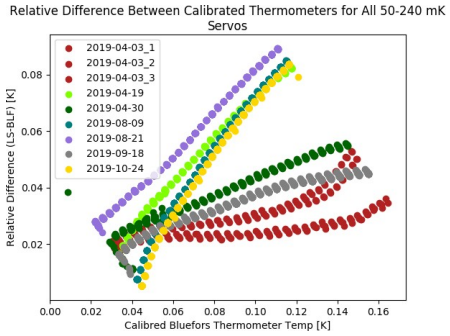

Figure 19: Overlay of servo section data for 7 DR cool downs. This plot overlays the same plot as in Figure 17 for 7 different cool downs. The formation of two different legs is evident, but there is no clear chronological pattern. For example, adjacent cooldowns on 4/19/2019 and 4/30/2019 exhibit completely different behavior. It should be noted that there are three different servo sections plotted for the 4/03/2019 cooldown because three different servos were executed in the same temperature range.

NEXT STEPS

I will continue to work on thermometry/timing housekeeping hardware for SO for the coming weeks. The bulk of my work will involve completing the planning, design, construction, and testing of the thermometry/timing enclosures for the SAT-1 housekeeping rack, and I plan to finish the same for the SAT-2 and SAT-3. I will also work to complete the design of the housekeeping rack enclosure and cooling system. Starting in September 2021 I will be moving to Princeton University to continue work on the Simons Observatory, finishing up projects begun at Yale and continuing on to the assembly and testing of a fourth SAT (the SAT-4) which will be fielded as part of a later stage of the observatory's operation.

ACKNOWLEDGEMENTS

I would like to thank Professor Laura Newburgh and Postdoctoral Researcher Brian Koopman for their mentorship and teaching. I would also like to thank undergraduate Sebastian Tsai for his help on various elements of my projects, and the Wright Laboratory support staff for help in machining and electrical work. Finally, a big thank you to YURA and the Yale Undergraduate Research Journal for the opportunity to share my work.

WORKS CITED

[1] Ali, Aamir, et al. "Studies of Systematic Uncertainties for Simons Observatory: Polarization Modulator Related Effects". Millimeter, Submillimeter, and Far-Infrared Detectors and Instrumentation for Astronomy IX, 2018, doi:10.1117/12.2312993.

[2] Ade, Peter, et al. (Simons Observatory Collaboration) "The Simons Observatory: Science Goals and Forecasts". 2018, pp. 2–4, The Simons Observatory: Science Goals and Forecasts.

[3] Duff, Shannon M. "Fabrication of 60,000+ transition edge sensor bolometers for the Simons Observatory." SPIE Conference. SPIE, Simons Observatory. Austin, Texas. June, 2018. Poster presentation.

[4] Koopman, B. J. "Detector Development and Polarization Analyses for the Atacama Cosmology Telescope." PhD Thesis, Cornell University, 2018.

[5] Kusaka, A. et al. "Modulation of Cosmic Microwave Background Polarization with a Warm Rapidly Rotating Half-Wave Plate on the Atacama B-Mode Search Instrument." Review of Scientific Instruments 85.2 (2014): 024501. Crossref. Web.

[6] Lee, Adrian, et al (Simons Observatory Collaboration). "The Simons Observatory: Astro2020 APC White Paper Project". 2019, arXiv:1907.08284.

[7] Ryden, Barbara. "Introduction to Cosmology". Cambridge University Press, 2017, pp. 147–152.

[8] "Epoch of Reionization". Historical Methods and Tools of Navigation, MIT Haystack Observatory, www.haystack.mit.edu/ast/science/epoch/.

[9] "BF-LD-Series Cryogen-Free Dilution Refrigerator System User Manual". Bluefors Cryogenics, INC., version 1.5.0, 2016.

[10] Ruthenium Oxide RTD Manual. Lakeshore Cryotronics, INC. https://www.lakeshore.com/docs/default-source/product-downloads/catalog/lstc$_$rox$_$l.pdf?sfvrsn=4ffff476$_$6.

[11] DT-670 Silicon Diode Manual. Lakeshore Cryotronics, INC. https://www.lakeshore.com/products/categories/overview/temperature-products/cryogenic-temperature-sensors/dt-670-silicon-diodes.

[12] "CMB Polarization." CMB Polarization, 5 Apr. 2016, www.cfa.harvard.edu/~cbischoff/cmb/.